Direct Synthesis of Functional Mesoporous Silica by Neutral pH Nonionic Surfactant Assembly: Factors Affecting Framework Structure and Composition

Roger Richer and Louis Mercier*

Department of Chemistry and Biochemistry, Laurentian University, Sudbury, Ontario, Canada P3E 2C6

Received April 10, 2001

The preparation of a wide range of organically functionalized wormhole-motif and hexagonal mesoporous MSU-X silicas was achieved by a one-step synthesis process involving the simultaneous addition of tetraethoxysilane (TEOS) and 3-mercaptopropyltrimethoxysilane (MPTMS) to solutions of structure-directing nonionic surfactant micelles, followed by fluoride-mediated hydrolysis/cross-linking and surfactant extraction. The effect of various synthesis parameters, including relative reagent concentration (MPTMS/TEOS ratio), temperature, and surfactant type, on the structure and composition of the mesostructures was investigated. Generally, higher MPTMS/TEOS ratios resulted in materials with higher functional group loadings, while increasing temperature also produced more highly functionalized materials. Although increasing synthesis temperature produced materials with greater pore diameters and lattice spacings, an increased organosilane content in the mesostructures produced materials with diminished pore diameters and lattice spacings. Thus, MSU-X materials with fine-tuned composition and pore dimensions were produced by systematically varying these synthesis parameters. We propose that the amphiphilic character of the nonionic surfactants is affected both by temperature and by the addition of the comparatively hydrophobic organosilane constituent in the micelle, thus forming mesostructures with corresponding compositional and structural features.

Introduction

The advent of mesostructure science has experienced an enormous surge of research activity since the introduction of M41S ordered mesoporous silica materials almost a decade ago.[1,2] Early pioneering work in this area found that ordered mesoporous oxides could be prepared by a cooperative assembly mechanism (denoted S^+I^- or S^-I^+) in which charged molecular metal oxide precursors (I^- or I^+) undergo cross-linking at the interface of surfactant micelles with hydrophilic headgroups bearing complementary charge (S^+ or S^-).[1−5] Since then, alternative mesostructure synthesis pathways have been demonstrated involving various surfactant−precursor assembly interactions, including counterion mediated interactions ($S^+X^-I^+$ or $S^-M^+I^-$),[3−5] complexation,[6,7] and liquid crystal templating.[8]

Two notable classes of mesostructured oxides have also been prepared using assembly mechanisms involving hydrogen-bonding interactions of neutral precursors with nonelectrostatic surfactants.[9−12] The first of these mechanisms, denoted S^0I^0, utilized primary alkylamines as structure-directing agents.[9,10] Silica mesostructures formed by this process were denoted HMS silica. The second nonelectrostatic mesostructure assembly route, denoted N^0I^0, involved the use of nonionic surfactants, including alkylpoly(ethylene oxide) diblock copolymer surfactant, bis(poly(ethylene oxide))polypropylene triblock copolymer surfactants, and ethoxylated sorbitan esters.[11−13] Siliceous materials formed by this pathway were designated as MSU-X materials. Using both S^0I^0 and N^0I^0 mechanisms, mesoporous materials related to those formed by electrostatic assembly are obtained, but with more disordered framework structures resulting

(1) Kresge, C. T.; Leonowicz, M. E.; Roth, W. J.; Vartuli, J. C.; Beck, J. S. *Nature* **1992**, *359*, 710.
(2) Beck, J. S.; Vartuli, J. C.; Roth, W. J.; Leonowicz, M. E.; Kresge, C. T.; Schmitt, K. D.; Chu, C. T.-W.; Olson, D. H.; Sheppard, E. W.; McCullen, S. B.; Higgins, J. B.; Schlenker, J. L. *J. Am. Chem. Soc.* **1992**, *114*, 10834.
(3) Monnier, A.; Schuth, F.; Huo, Q.; Kumar, D.; Margolese, D.; Maxwell, R. S.; Stucky, G. D.; Krishnamurty, M.; Petroff, P.; Firouzi, A.; Janicke, M.; Chmelka, B. F. *Science* **1993**, *261*, 1299.
(4) Huo, Q.; Margolese, D. I.; Ciesla, U.; Feng, P.; Gier, T. E.; Sieger, P.; Leon, R.; Petroff, P. M.; Schuth, F.; Stucky, G. D. *Nature* **1994**, *368*, 317.
(5) Huo, Q.; Margolese, D. I.; Ciesla, U.; Demuth, D. G.; Feng, P.; Gier, T. E.; Sieger, P.; Firouzi, A.; Chmelka, B. F.; Schuth, F.; Stucky, G. D. *Chem. Mater.* **1994**, *6*, 1176.
(6) Antonelli, D. M.; Ying, J. Y. *Angew. Chem., Int. Ed. Engl.* **1996**, *35*, 426.
(7) Antonelli, D. M.; Ying, J. Y. *Chem. Mater.* **1996**, *8*, 874.
(8) Attard, G. S.; Glyde, J. C.; Göltner, C. G. *Nature* **1995**, *378*, 366.
(9) Tanev, P. T.; Pinnavaia, T. J. *Science* **1995**, *267*, 865.
(10) Tanev, P. T.; Pinnavaia, T. J. *Chem. Mater.* **1996**, *8*, 2068.
(11) (a) Bagshaw, S. A.; Prouzet, E.; Pinnavaia, T. J. *Science* **1995**, *269*, 1242. (b) Bagshaw, S. A.; Kemmitt, T.; Milestone, N. *Microporous Mesoporous Mater.* **1998**, *22*, 419. (c) Bagshaw, S. A. *J. Mater. Chem.* **2001**, *11*, 831.
(12) (a) Prouzet, E.; Pinnavaia, T. J. *Angew. Chem., Int. Ed. Engl.* **1997**, *36*, 516. (b) Boissière, C.; van der Lee, A.; El Mansouri, A.; Larbot, A.; Prouzet, E. *Chem Commun.* **1999**, 2047. (c) Boissière, C.; Larbot, A.; van der Lee, A.; Kooyman, P. J.; Prouzet, E. *Chem. Mater.* **2000**, *12*, 2902. (d) Boissière, C.; Larbot, A.; Prouzet, E. *Chem. Mater.* **2000**, *12*, 1937.
(13) Prouzet, E.; Cot, F.; Nabias, G.; Larbot, A.; Kooyman, P.; Pinnavaia, T. J. *Chem. Mater.* **1999**, *11*, 1498.

10.1021/cm010295v CCC: $20.00
Published on Web 08/29/2001

in wormhole-motif pore channel structures. An unprecedented feature of N^0I^0 assembly is the ability to control the amphiphilic character of the nonionic surfactant micelles by varying the temperature.[12] This property, essentially causing the hydrophobic core of the micelles to swell in size as a function of increasing temperature, was exploited by Prouzet and Pinnavaia in order to produce mesoporous silica with pore diameters that systematically increase as a function of the synthesis temperature used in their preparation.[12]

To render mesostructured materials suitable for practical applications, the preparation of functionalized derivatives of surfactant-assembled silica mesostructures has been widely investigated in recent years. Early attempts at the functionalization of mesostructured oxides involved the use of postsynthesis grafting, wherein moieties are tethered onto preformed mesostructure frameworks.[14−22] The grafting of various moieties inside the pore channels of these frameworks produced materials promising for a multitude of applications, particularly for catalysis[14,15,17−19] and adsorption.[21,22]

To allow greater control over functional group loading and surface uniformity, significant research efforts have been invested to producing functionalized mesostructures by one-step synthesis procedures, following a *direct incorporation* process.[23−36] Thus, the simultaneous addition of tetraalkoxysilane and organotrialkoxysilane precursors directly into mesostructure synthesis mixtures containing ionic surfactants (i.e., alkyltrimethylammonium salts) produced functionalized analogues of MCM-41.[23−29] The use of nonelectrostatic surfactants as structure-directing agents was also investigated to provide alternate synthesis routes to such organosilica mesostructures.[30−36] Thus, functionalized HMS[30−34] and MSU-X[35,36] silica analogues were prepared using primary alkylamine and nonionic surfactant structure directors.

The one-step preparation of functionalized HMS and MSU-X materials by nonelectrostatic surfactant assembly provides many synthetic advantages over the more ubiquitous electrostatic assembly method. For instance, the assembly of functional HMS and MSU-X mesostructures can be performed under neutral or near-neutral pH conditions,[30−36] as opposed to the much harsher extreme pH conditions (typically alkaline) associated with the preparation of MCM-41-type materials.[23−29] Moreover, the use of uncharged structure-directing surfactants allows their complete removal from the pore channels by nondestructive solvent extraction methods. Like their pure silica analogues, the functionalized HMS and MSU-X materials do not exhibit the high degree of crystallographic order as their electrostatically assembled MCM-41 counterparts (i.e., they have wormhole-motif structure), although these frameworks nonetheless possess uniform nanometer-sized pore channels typical of surfactant-assembled oxides.

Recently, Mercier and Pinnavaia reported an extensive investigation on the direct incorporation of various functional groups inside the framework of HMS silica (using neutral alkylamines as structure-directing agents).[34] Although it was demonstrated that judicious control over the structure and function of modified HMS silica could be achieved by this technique, the nucleophilicity of the alkylamine surfactant makes the technique unsuitable for the inclusion of highly electrophilic functional groups (such as halogenoalkanes). Richer and Mercier have also shown that neutral pH nonionic surfactant assembly (N^0I^0) can also be used to form functional mesostructured MSU-X derivatives in a one-step process.[35] A clear advantage associated with this latter method is the chemical inertness of the surfactant, which can allow the incorporation of functional groups that might otherwise not withstand the assembly conditions used either in electrostatic assembly or in HMS synthesis.

In this paper, we report an extensive study of the effect of various synthesis parameters on the structure and function of derivatized MSU-X mesostructures prepared by a one-step neutral pH process. Mercaptopropyl groups ($CH_2CH_2CH_2SH$) have been selected as the incorporated functional moiety (a "probe" moiety) for all the experiments shown, since sulfur could be accurately assayed using readily available instrumentation. Moreover, thiol-functionalized mesostructures have in recent years attracted much attention as highly effective heavy metal ion adsorbents,[21,22,36−38] making these materials exceptionally promising for environmental remediation applications.

Experimental Section

Materials. All chemicals were purchased from Aldrich and used without further purification. Deionized water and 95% ethanol were used in the syntheses and extraction processes, respectively.

(14) Tanev, P. T.; Chibwe, M.; Pinnavaia, T. J. *Nature* **1994**, *368*, 321.
(15) Maschmeyer, T.; Rey, F.; Sankar, G.; Thomas, J. M. *Nature* **1995**, *378*, 159.
(16) Brunel, D.; Cauvel, A.; Fajula, F.; DiRenzo, F. *Stud. Surf. Sci. Catal.* **1995**, *97*, 173.
(17) Zhang, W.; Pinnavaia, T. J. *Catal. Lett.* **1996**, *38*, 261.
(18) Zhang, W.; Wang, J.; Tanev, P. T.; Pinnavaia, T. J. *J. Chem. Soc., Chem. Commun.* **1996**, 979.
(19) Zhang, W.; Froba, M.; Wang, J.; Tanev, P. T.; Wong, J.; Pinnavaia, T. J. *J. Am. Chem. Soc.* **1996**, *118*, 9164.
(20) Cauvel, A.; Brunel, D.; Renzo, F. D.; Fajula, F. *AIP Conf. Proc.* **1996**, *354*, 477.
(21) Mercier, L.; Pinnavaia, T. J. *Adv. Mater.* **1997**, *9*, 500.
(22) Feng, X.; Fryxell, G. E.; Wang, L.-Q.; Kim, A. Y.; Liu, J.; Kemner, K. M. *Science* **1997**, *276*, 923.
(23) Burkett, S. L.; Sims, S. D.; Mann, S. J. *J. Chem. Soc., Chem. Commun.* **1996**, 1367.
(24) Lim, M. H.; Blanford, C. F.; Stein, A. *J. Am. Chem. Soc.* **1997**, *119*, 4090.
(25) Fowler, C. E.; Burkett, S. L.; Mann, S. J. *Chem. Commun.* **1997**, 1769.
(26) Lim, M. H.; Blanford, C. F.; Stein, A. *Chem. Mater.* **1998**, *10*, 467.
(27) Van Rhijn, W. M.; DeVos, D. E.; Sels, B. F.; Bossaert, W. D.; Jacobs, P. A. *Chem. Commun.* **1998**, 317.
(28) Babonneau, F.; Leite, L.; Fontlupt, S. *J. Mater. Chem.* **1999**, *9*, 175.
(29) Hall, S. R.; Fowler, C. E.; Lebeau, B.; Mann, S. *Chem. Commun.* **1999**, 201.
(30) Macquarrie, D. J. *Chem. Commun.* **1996**, 1961.
(31) Macquarrie, D. J.; Jackson, D. B.; Mdoe, J. E. G.; Clark, J. H. *New J. Chem.* **1999**, *23*, 539.
(32) Corriu, R. J. P.; Mehdi, A.; Reyé, C. *C. R. Acad. Sci. Ser. II C* **1999**, *2*, 35.
(33) Bossaert, W. D.; De Vos, D. E.; Van Rhijn, W. M.; Bullen, J.; Grobet, P. J.; Jacobs, P. A. *J. Catal.* **1999**, *182*, 156.
(34) Mercier, L.; Pinnavaia, T. J. *Chem. Mater.* **2000**, *12*, 188.
(35) Richer, R.; Mercier, L. *J. Chem. Soc., Chem. Commun.* **1998**, 1775.
(36) Brown, J.; Richer, R.; Mercier, L. *Micropor. Mesopor. Mater.* **2000**, *37*, 41.
(37) Mercier, L.; Pinnavaia, T. J. *Environ. Sci. Technol.* **1998**, *32*, 2749.
(38) Brown, J.; Mercier, L.; Pinnavaia, T. J. *Chem. Commun.* **1999**, 69.

Table 1. Physicochemical Characteristics of Mercaptopropyl-Functionalized MSU-2 Mesostructures Formed Using Igepal CA-720 as the Structure-Directing Surfactant

material designation	*T* (°C)	mol % MPS in soln	mol % MPS in mater	BET surf. area ($m^2\ g^{-1}$)	pore vol ($cm^3\ g^{-1}$)	pore diam (Å)	d_{100} (Å)	wall thickness (Å)	% yield
MSU-2-15(IG)	15	0.0	0.0	1326	0.67	29	46.4	17	92
MP-MSU-2-1.0-15(IG)	15	1.0	0.7	1317	0.68	29	46.0	17	96
MP-MSU-2-2.0-15(IG)	15	2.0	1.6	1452	0.71	28	44.6	17	78
MP-MSU-2-3.0-15(IG)	15	3.0	2.3	1396	0.68	28	45.0	17	100
MP-MSU-2-4.0-15(IG)	15	4.0	3.4	1356	0.62	27	43.0	16	99
MP-MSU-2-5.0-15(IG)	15	5.0	4.1	1336	0.62	27	43.5	17	88
MSU-2-30(IG)	30	0.0	0.0	1012	0.49	28	47.4	19	54
MP-MSU-2-1.0-30(IG)	30	1.0	0.8	1145	0.53	27	45.8	19	55
MP-MSU-2-2.0-30(IG)	30	2.0	1.6	951	0.41	26	42.6	17	36
MP-MSU-2-3.0-30(IG)	30	3.0	3.2	1291	0.59	26	50.0	24	51
MP-MSU-2-4.0-30(IG)	30	4.0	4.9	918	0.40	25	44.7	20	42
MP-MSU-2-5.0-30(IG)	30	5.0	6.2	1108	0.46	24	40.1	16	36
MSU-2-40(IG)	40	0.0	0.0	1012	0.86	35	48.8	14	43
MP-MSU-2-1.0-40(IG)	40	1.0	1.4	1382	0.86	34	46.0	12	40
MP-MSU-2-2.0-40(IG)	40	2.0	3.6	1442	0.74	33	45.3	12	39
MP-MSU-2-3.0-40(IG)	40	3.0	5.8	1323	0.73	30	45.0	15	39
MP-MSU-2-4.0-40(IG)	40	4.0	7.6	781	0.31	24	37.7	14	40
MP-MSU-2-5.0-40(IG)	40	5.0	8.7	780	0.32	22	38.8	17	43
MSU-2-50(IG)	50	0.0	0.0	918	0.55	38	49.1	15	34
MP-MSU-2-1.0-50(IG)	50	1.0	2.0	1035	0.58	34	49.1	15	32
MP-MSU-2-2.0-50(IG)	50	2.0	4.6	1044	0.55	33	49.1	16	29
MP-MSU-2-3.0-50(IG)	50	3.0	6.1	964	0.49	30	51.9	22	35
MP-MSU-2-4.0-50(IG)	50	4.0	7.8	886	0.51	24	42.2	18	27
MP-MSU-2-5.0-50(IG)	50	5.0	10.5	739	0.28	22	40.3	18	36

Mesostructure Synthesis. The synthesis of functionalized MSU-X materials was performed following a procedure modified from that initially developed by Bagshaw, Prouzet, and Pinnavaia.[11a,12] In a typical preparation, a mixture of tetraethoxysilane (TEOS) and 3-mercaptopropyltrimethoxysilane (MPTMS) was added to 100 mL of a stirred solution of a nonionic surfactant. The nonionic surfactants used and their respective concentrations were as follows: Tergitol 15-S-12 ($C_{15}H_{31}(OCH_2CH_2)_{10}OH$), 2.0×10^{-2} M; Triton-X100 ($C_8H_{17}C_6H_5(OCH_2CH_2)_8OH$), 2.7×10^{-2} M; Igepal CA-720 ($C_8H_{17}C_6H_5(OCH_2CH_2)_{10}OH$), 2.7×10^{-2} M; Brij-76 ($C_{18}H_{37}(OCH_2CH_2)_{10}OH$), 2.7×10^{-2} M. The surfactant:TEOS:MPTMS molar composition of each synthesis mixture was $1.0{:}8.0 - X{:}X$, where X was varied between 0 and 0.4 (representing MPTMS/(TEOS + MPTMS) molar ratios ranging from 0 to 0.05). The open beaker containing the initially immiscible mixture was placed in a water bath with a controlled temperature of 15 °C and stirred until a clear solution was obtained. At that point, 8.6×10^{-4} mol NaF was added to the solution to instigate the cross-linking of the silica framework.[12] After aging for 4 h, the product was filtered and air-dried and the framework-bound surfactant was removed by Soxhlet extraction over ethanol for 24 h.

The procedure described above was repeated for each surfactant at synthesis temperatures of 30, 40, and 50 °C. Owing to its insolubility at low temperatures, the Brij-76 assembly system was instead prepared at synthesis temperatures of 40 and 60 °C.

Mesostructure Characterization. Powder X-ray diffraction patterns were measured on a Rigaku Rotaflex diffractometer equipped with a rotating anode and using Cu Kα radiation (Ontario Geoscience Laboratories, Sudbury, Ontario, Canada).

N_2 adsorption isotherms of the adsorbents were measured at −196 °C on a Micromeritics ASAP 2010 sorptometer. Prior to measurement, all samples were outgassed at 110 °C at 10^{-6} mmHg. BET surface areas were measured from the linear part of the BET plot ($0.05 < P/P_0 < 0.25$). Mesopore volumes (V_{mp}) were assumed to be equal to the liquid volume of adsorbed nitrogen below $P/P_0 = 0.7$. Pore size distributions were calculated using the Olivier−Conklin density functional theory (DFT) method.[39]

The sulfur content in the materials was determined using a LECO IR 32H sulfur determinator (Central Analytical Facility, Laurentian University).

Proton-decoupled ^{29}Si MAS NMR spectra were recorded on a Bruker AMX 200 MHz spectrometer at 39.8 MHz, with a pulse delay of 300 s to ensure full relaxation of the nuclei prior to each scan (University of Ottawa NMR Laboratory).

Transmission electron microscopy (TEM) images of the mesostructures were obtained from ultrathin sections (∼50 nm) of epoxy resin-embedded samples (IMAGETEK Analytical Imaging, Toronto, Ontario, Canada).

Scanning electron microscopy (SEM) images of the adsorbents were obtained using a JEOL JSM6400 scanning electron microscope (Ontario Geosciences Laboratories).

Results and Discussion

The physical and chemical characteristics of all synthesized mesostructures are shown in Tables 1−4. The designations of the materials (first column, Tables 1−4) were made according to their mesostructure prototype, their incorporated functional group (MPTMS), the amount of functional group (MPTMS) used for their preparation (third column, Tables 1−4), their synthesis temperature (second column, Tables 1−4), and the surfactant used for their assembly. For example, a sample designated as "MP-MSU-1-1.0-30(TG)" would consist of an MSU-1 structure functionalized with mercaptopropyl (MP) moieties (N.B., according to the designation system established in ref 11a, Tergitol and Brij surfactants form MSU-1 structures since their hydrophobic hydrocarbon tails are aliphatic, whereas mesostructures assembled using Triton and Igepal surfactants are labeled MSU-2 because of the presence of phenyl rings in their hydrophobic tails). The number "1.0" in the designation denotes that 1.0% of the total silane used in the material's initial synthesis mixture was in the form of mercaptopropyltrimethoxysilane (MPTMS) (i.e., the molar ratio of MPTMS/(MPTMS + TEOS) in the synthesis mixture is equal to 0.010). Last,

(39) *Analytical Methods in Fine Particle Technology*; Webb, P. A., Orr, C., Eds.; Micromeritics Instrument Corporation, Norcross, GA, 1997; pp 81−87.

Table 2. Physicochemical Characteristics of Mercaptopropyl-Functionalized MSU-1 Mesostructures Formed Using Tergitol 15-S-12 as the Structure-Directing Surfactant

material designation	*T* (°C)	mol % MPS in soln	mol % MPS in mater	BET surf. area ($m^2\ g^{-1}$)	pore vol ($cm^3\ g^{-1}$)	pore diam (Å)	d_{100} (Å)	wall thickness (Å)	% yield
MSU-1-15(TG)	15	0.0	0.0	1274	0.61	28	41.5	14	72
MP-MSU-1-0.5-15(TG)	15	0.5	0.2	1054	0.44	25	40.3	15	67
MP-MSU-1-1.0-15(TG)	15	1.0	0.5	1643	0.76	28	42.0	14	67
MP-MSU-1-2.0-15(TG)	15	2.0	1.1	1238	0.60	27	42.9	16	54
MP-MSU-1-3.0-15(TG)	15	3.0	2.1	1247	0.57	27	42.2	15	60
MSU-1-30(TG)	30	0.0	0.0	768	0.80	45	50.9	6	50
MP-MSU-1-1.0-30(TG)	30	1.0	1.6	935	0.90	43	48.8	6	44
MP-MSU-1-2.0-30(TG)	30	2.0	3.1	815	0.58	36	48.2	12	44
MP-MSU-1-3.0-30(TG)	30	3.0	4.8	888	0.59	35	46.6	12	45
MSU-1-40(TG)	40	0.0	0.0	1031	0.54	32	48.8	17	38
MP-MSU-1-0.5-40(TG)	40	0.5	0.8	952	0.67	38	50.9	13	40
MP-MSU-1-1.0-40(TG)	40	1.0	2.2	1277	0.68	33	47.1	14	61
MP-MSU-1-2.0-40(TG)	40	2.0	2.9	1212	0.61	29	46.1	17	64
MP-MSU-1-3.0-40(TG)	40	3.0	3.0	1107	0.48	26	43.1	17	52
MSU-1-50(TG)	50	0.0	0.0	969	0.84	44	54.0	10	30
MP-MSU-1-0.5-50(TG)	50	0.5	1.4	1052	0.78	40	53.3	13	29
MP-MSU-1-1.0-50(TG)	50	1.0	2.8	1042	0.68	36	53.7	18	31
MP-MSU-1-2.0-50(TG)	50	2.0	4.3	1121	0.66	35	50.3	15	39

Table 3. Physicochemical Characteristics of Mercaptopropyl-Functionalized MSU-2 Mesostructures Formed Using Triton-X100 as the Structure-Directing Surfactant

material designation	*T* (°C)	mol % MPS in soln	mol % MPS in mater	BET surf. area ($m^2\ g^{-1}$)	pore vol ($cm^3\ g^{-1}$)	pore diam (Å)	d_{100} (Å)	wall thickness (Å)	% yield
MSU-2-15(TX)	15	0.0	0.0	854	0.45	35	60.0	25	98
MP-MSU-2-0.5-15(TX)	15	0.5	0.2	826	0.42	35	54.0	19	58
MP-MSU-2-1.0-15(TX)	15	1.0	0.3	826	0.43	36	57.1	21	92
MP-MSU-2-2.0-15(TX)	15	2.0	1.2	711	0.30	23			77
MP-MSU-2-3.0-15(TX)	15	3.0	2.2	622	0.26	20			77
MSU-2-30(TX)	30	0.0	0.0	905	0.93	43	48.8	6	22
MP-MSU-2-0.5-30(TX)	30	0.5	0.5	1065	0.80	38	47.7	10	29
MP-MSU-2-1.0-30(TX)	30	1.0	1.4	934	0.81	38	47.4	9	31
MP-MSU-2-2.0-30(TX)	30	2.0	3.1	1405	0.71	29			31
MP-MSU-2-3.0-30(TX)	30	3.0	4.9	1264	0.67	29	43.6	15	34
MSU-2-40(TX)	40	0.0	0.0	966	0.91	58	69.8	12	43
MP-MSU-2-0.5-40(TX)	40	0.5	0.9	1082	0.87	52	68.1	16	43
MP-MSU-2-1.0-40(TX)	40	1.0	1.8	1067	0.81	48	66.9	19	41
MP-MSU-2-2.0-40(TX)	40	2.0	3.2	862	0.38	24			44
MP-MSU-2-3.0-40(TX)	40	3.0	5.0	940	0.50	27,34			44
MSU-2-50(TX)	50	0.0	0.0	721	0.84	55	65.3	10	7
MP-MSU-2-0.5-50(TX)	50	0.5	1.6	739	1.00	60	75.7	16	20
MP-MSU-2-1.0-50(TX)	50	1.0	2.2	937	1.01	50	69.2	19	32
MP-MSU-2-2.0-50(TX)	50	2.0	5.1	1020	0.87	46	61.4	15	28
MP-MSU-2-3.0-50(TX)	50	3.0	5.9	1061	0.89	43	60.9	18	37

Table 4. Physicochemical Characteristics of Mercaptopropyl-Functionalized MSU-1 Mesostructures Formed Using Brij-76 as the Structure-Directing Surfactan

material designation	*T* (°C)	mol % MPS in soln	mol % MPS in mater	BET surf. area ($m^2\ g^{-1}$)	pore vol ($cm^3\ g^{-1}$)	pore diam (Å)	d_{100} (Å)	wall thickness (Å)	% yield
MSU-1-40(BJ)	40	0.0	0.0	1253	1.37	54	63.5	19[a]	59
MP-MSU-1-1.0-40(BJ)	40	1.0	2.2	1461	1.46	51	64.4	23[a]	56
MP-MSU-1-2.0-40(BJ)	40	2.0	4.0	1102	1.10	47	61.7	24[a]	53
MP-MSU-1-3.0-40(BJ)	40	3.0	4.9	1187	1.17	46	60.4	24[a]	58
MP-MSU-1-4.0-40(BJ)	40	4.0	6.0	1216	1.15	46	58.4	21[a]	59
MP-MSU-1-5.0-40(BJ)	40	5.0	7.0	1349	1.20	43	58.8	25[a]	58
MSU-1-60(BJ)	60	0.0	0.0	630	0.53	69	78.8	10	20
MP-MSU-1-1.0-60(BJ)	60	1.0	2.9	1047	0.91	64	81.0	17	23
MP-MSU-1-2.0-60(BJ)	60	2.0	4.9	1212	1.19	57	79.3	22	17
MP-MSU-1-3.0-60(BJ)	60	3.0	6.6	910	0.90	54	75.4	21	18
MP-MSU-1-4.0-60(BJ)	60	4.0	8.1	771	0.77	54	81.0	27	22
MP-MSU-1-5.0-60(BJ)	60	5.0	9.5	812	0.76	49	81.0	32	24

[a] Due to the hexagonal symmetry of the lattice, wall thickness $= 2d_{100}/\sqrt{3}$ − pore diameter.

the number "30" refers to the synthesis temperature of the material (in °C), and "TG" specifies the assembly surfactant used (viz., in this paper we have used TG to denote Tergitol 15-S-12, TX for Triton-X100, IG for Igepal CA-720, and BJ for Brij-76).

The fourth column in Tables 1−4 refers to the molar percentage of functional group (i.e., mercaptopropylsilyl groups, hereafter denoted MPS) incorporated into the mesostructure frameworks. These values have been determined on the basis of the chemical compositions

of the materials deduced from ^{29}Si MAS NMR and S content analyses. The ^{29}Si MAS NMR spectra of the mesostructures showed the presence of the following Si sites: Q^4 signals at −110 ppm ($(SiO)_4Si$), Q^3 signals at −101 ppm ($(SiO)_3SiOH$) (both corresponding to framework silica derived from hydrolyzed TEOS), and T^2 ($(SiO)_2Si(OH)(CH_2)_3SH$) and T^3 ($(SiO)_3Si(CH_2)_3SH$) signals (at −60 and −65 ppm, respectively) corresponding to the organosilane (mercaptopropylsilane, MPS) silicon atoms. The Q^4/Q^3 signal intensity ratio in every material studied was always close to 2.0, while the intensity of the T^2 signal was negligeable compared to that of the T^3 signal. The following approximate general chemical formula was thus proposed for the mercaptopropyl-functionalized mesostructures:

$$[(SiO_2)_{0.67}(SiO_{2.5}H)_{0.33}]_{1-n}[SiO_{1.5}(CH_2)_3SH]_n$$

where n represents the molar fraction of organosilane moieties in the materials with respect to the total Si in the mesostructure. Because the organosilane contents in the mesostructures prepared in this work were relatively small, an accurate determination of the n value for these materials could not be done by ^{29}Si NMR data alone because of the weak organosilane T^3 signals. Thus, sulfur analysis was used to obtain more accurate n values for the mesostructures. Hence, the numbers shown on the fourth column in Tables 1−4 are equal to $100n$ (i.e., the molar percentage of organosilane (MPS) in the mesostructure framework).

The framework wall thickness for each mesostructure (column 9 in Tables 1−4) was determined by subtracting its pore diameter (column 7 in Tables 1−4) from its average pore-center-to-pore-center distance (assumed to be equal to the materials' d_{100} spacings in the case of disordered wormhole motif mesostructures,[12,13] column 8 in Tables 1−4).

General Features of Synthesized Materials. Most of the materials synthesized in this work possessed XRD patterns with appearances typical of those of an MSU-X wormhole-motif mesostructure, featuring a single correlation reflection at 2θ angles usually between 1° and 3° (Figure 1).[11−13] The corresponding N_2 isotherms of the materials featured sharp inflections in the intermediate P/P_0 region, indicating the presence of uniform mesopore channels (Figure 2). The very high surface areas (generally in the range 700−1400 $m^2\ g^{-1}$) and pore volumes (generally in the range 0.40−1.20 $cm^3\ g^{-1}$) measured from these isotherms (Tables 1−4) were also characteristic of mesostructured materials.[1−38,40] Based on the isotherm data of these materials, very narrow mesopore size distributions (with maxima in the range 20−60 Å) were determined for these materials (Figure 3, Tables 1−4), once again consistent with the expected properties of mesostructured materials.[1−38,40] The framework wall thicknesses of the materials (Tables 1−4) generally ranged from about 10 to 25 Å, with the more highly MPS-loaded materials generally having thicker walls owing to the presence of the functional groups on the surface of the pore channels.

Electron micrographs of representative mesostructure samples showed that these consisted of ultrafine spherical particles with diameters in the range 0.4−1.2 μm (Figure 4a). Higher resolution images of the samples revealed that these consisted entirely of wormhole-motif mesostructured frameworks, with no amorphous silica being observed (Figure 4b).

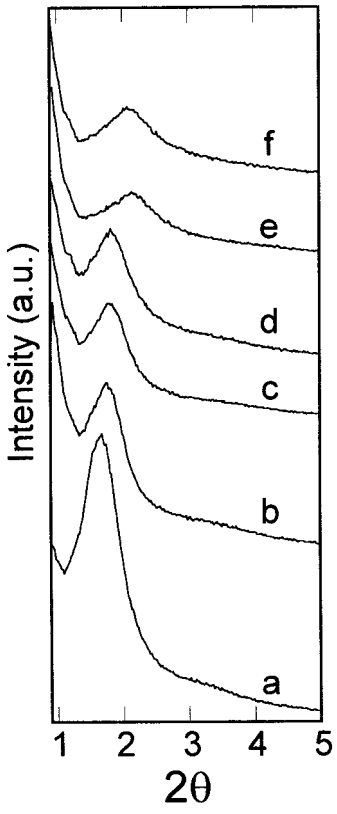

Figure 1. Powder X-ray diffraction patterns for MSU-2 and its functionalized derivatives formed using Igepal CA-720 as structure-directing surfactant at 40 °C: (a) MSU-2-40(IG), (b) MP-MSU-2-1.0-40(IG), (c) MP-MSU-2-2.0-40(IG), (d) MP-MSU-2-3.0-40(IG), (e) MP-MSU-2-4.0-40(IG), and (f) MP-MSU-2-5.0-40(IG).

Unlike the other materials synthesized in this work, the mesostructures prepared using Brij-76 at a temperature of 40 °C produced highly ordered materials with XRD patterns typical of mesostructures with hexagonal space symmetry (i.e., MCM-41, SBA), with sharp (100), (110), and (200) reflections being clearly observed (Figure 5).[1−5,40] The N_2 isotherms (Figure 6) and narrow pore size distributions (Figure 7) of these materials were also characteristic of mesoporous material with highly uniform pore channels. The hexagonal order in these materials is clearly seen in their transmission electron micrographs (Figure 8, bottom), and virtually no amorphous material can be seen in the samples. The microscale morphology of these materials were, moreover, different from that of the wormhole-motif materials prepared using Triton-X, Tergitol, and Igepal surfactants: instead of submicrometric spheres, these were shaped like short "spaghetti strand" rods (Figure 8, top). The structural features of these mesostructures were reminiscent of those reported by Boissière et al., who obtained hexagonal mesostructures with rodlike particle morphologies using Pluronic P-123 as a structure-directing surfactant.[12b] The authors of the latter work ascribed the formation of these highly ordered fibrous structures to the decreased hydrophilicity of the Pluronic P-123 surfactant compared to linear surfactants

(40) Zhao, D.; Huo, Q.; Feng, J.; Chmelka, B. F.; Stucky, G. D. *J. Am. Chem. Soc.* **1998**, *120*, 6024.

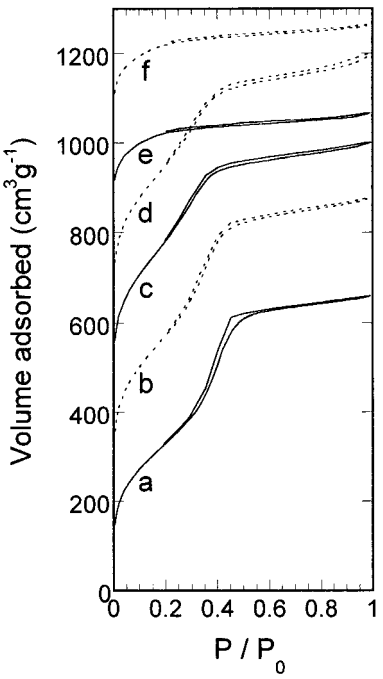

Figure 2. N_2 adsorption−desorption isotherms for MSU-2 and its functionalized derivatives formed using Igepal CA-720 as structure-directing surfactant at 40 °C: (a) MSU-2-40(IG), (b) MP-MSU-2-1.0-40(IG), (c) MP-MSU-2-2.0-40(IG), (d) MP-MSU-2-3.0-40(IG), (e) MP-MSU-2-4.0-40(IG), and (f) MP-MSU-2-5.0-40(IG). For the sake of clarity, the isotherms have been offset by 200 cm^3 g^{-1} along the volume adsorbed axis.

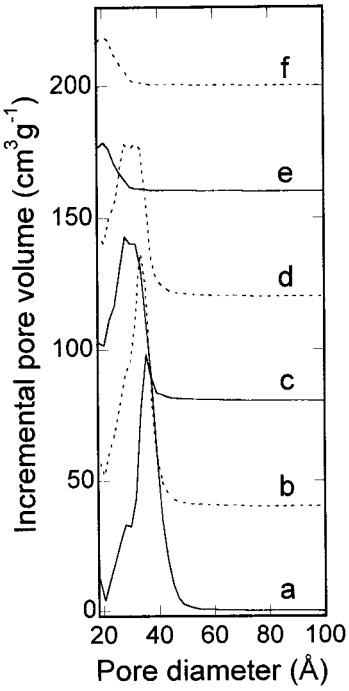

Figure 3. Pore size distributions for MSU-2 and its functionalized derivatives formed using Igepal CA-720 as structure-directing surfactant at 40 °C: (a) MSU-2-40(IG), (b) MP-MSU-2-1.0-40(IG), (c) MP-MSU-2-2.0-40(IG), (d) MP-MSU-2-3.0-40(IG), (e) MP-MSU-2-4.0-40(IG), and (f) MP-MSU-2-5.0-40(IG).

such as Tergitol 15-S-12.[12b] A similar observation can be made regarding Brij-76, which has a substantially longer hydrophobic tail than those of the other surfactants used in this study and is thus less hydrophilic than Tergitol 15-S12, Triton-X100, and Igepal CA-720.

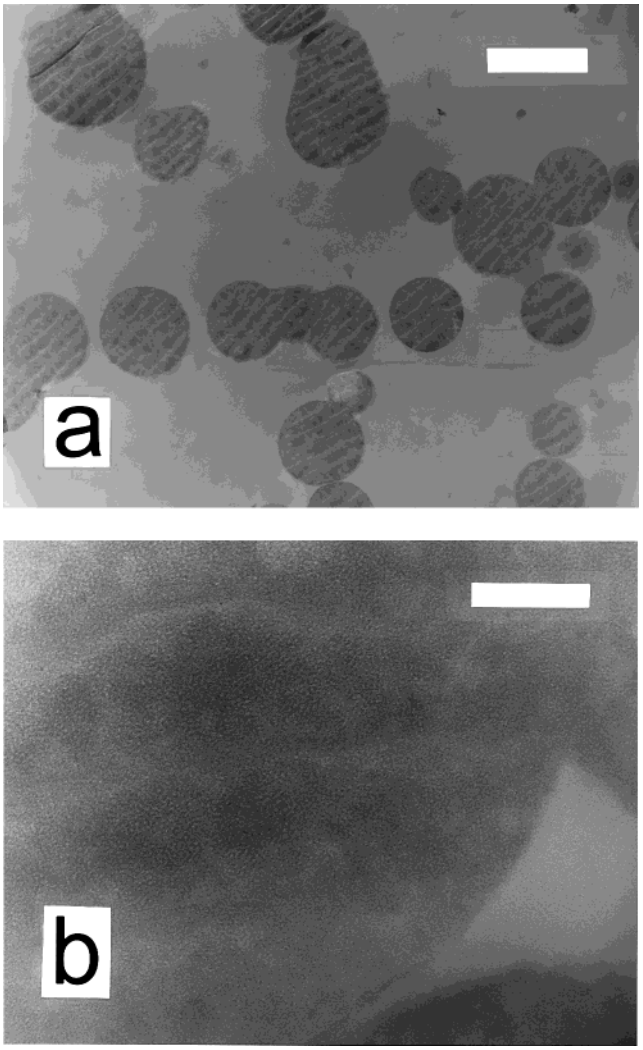

Figure 4. (a) Low magnification (scale bar = 1 μm) and (b) high magnification (scale bar = 100 nm) transmission electron micrographs of a mesostructure (MP-MSU-2-2.0-40(IG)) assembled using Igepal CA-720.

Interestingly, the mesostructures prepared using Brij-76 at 60 °C reverted to wormhole-motif structures similar to those of the MSU-X compounds prepared using Tergitol, Triton-X, or Igepal structure directors.[11,12] We postulate that the hexagonal ordering resulting from the 40 °C synthesis may be linked to the fact that Brij-76 only becomes completely soluble in water at a temperature of about 40 °C. At this temperature, the proximity to the surfactant's solubility limit may result in the formation of very rigid liquid crystal-like micellar rods in solution, producing highly ordered hexagonal mesostructures reminiscent of SBA-type materials prepared using nonionic surfactants under highly acidic conditions.[40] When the temperature is increased beyond this point, the micelles revert to the wormlike structure typical of nonionic surfactants in nonacidic aqueous media and the more ubiquitous MSU-1 silica structure type is obtained.

Effect of Synthesis Parameters on Chemical Composition. Predictably, the amount of MPS moieties incorporated within the framework of the MSU-X mesostructures was found to vary (at any given temperature and for any given surfactant) in direct proportion to the relative amount of MPTMS used in the original

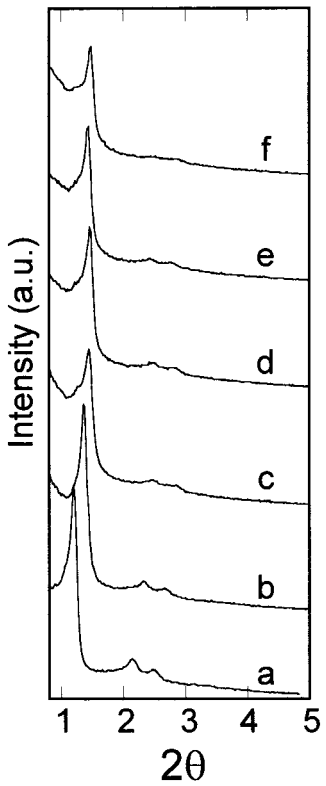

Figure 5. Powder X-ray diffraction patterns for MSU-1 and its functionalized derivatives formed using Brij-76 as structure-directing surfactant at 40 °C: (a) MSU-1-40(BJ), (b) MP-MSU-1-1.0-40(BJ), (c) MP-MSU-1-2.0-40(BJ), (d) MP-MSU-1-3.0-40(BJ), (e) MP-MSU-1-4.0-40(BJ), and (f) MP-MSU-1-5.0-40(BJ).

synthesis mixture (with respect to TEOS) (Tables 1−4).[34] However, the molar compositions of the materials *do not* necessarily correspond exactly to that which would be expected based on the relative MPTMS:TEOS ratio used to synthesize the materials. Moreover, the synthesis yields of the mesostructures were typically not quantitative, with higher synthesis temperatures generally reducing the overall yields (Tables 1−4). In contrast to these observations, the composition of organically modified HMS silicas prepared by direct organosilane incorporation was found to mirror that of the original synthesis mixture, and near quantitative synthesis yields were obtained.[34]

At any given synthesis mixture composition, the increase of the synthesis temperature resulted in an increase in the MPS content of the resulting mesostructure (Tables 1−4). Figure 9 graphically illustrates the combined effects of both temperature and initial solution composition on the functional group loading of MSU-2 silica prepared using Igepal CA-720 as the surfactant, and demonstrates the ability of neutral pH nonionic surfactant assembly to achieve a judicious control of organo-mesostructure composition by varying either (or both) of these parameters.

Formation Mechanism of MPS-Incorporated Mesostructures. We propose that the increased MPS loading in the materials prepared at higher temperature results from the swelling of the hydrophobic core of nonionic surfactant micelles at higher temperatures.[12] The formation of MP-MSU-X materials first requires the dissolution of both TEOS and MPTMS inside the structure-directing micelles, followed by the evaporation

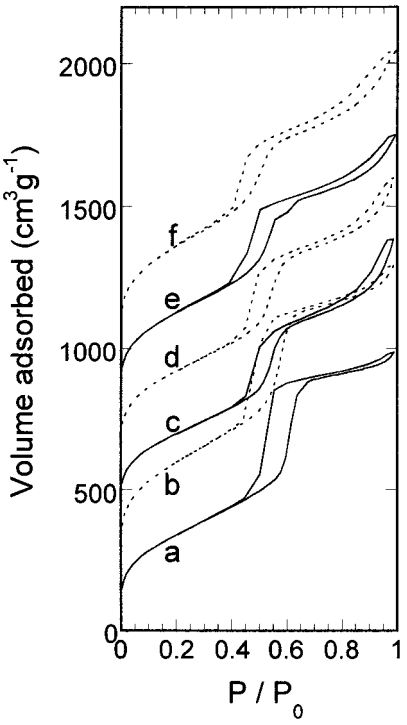

Figure 6. N_2 adsorption−desorption isotherms for MSU-1 and its functionalized derivatives formed using Brij-76 as structure-directing surfactant at 40 °C: (a) MSU-1-40(BJ), (b) MP-MSU-1-1.0-40(BJ), (c) MP-MSU-1-2.0-40(BJ), (d) MP-MSU-1-3.0-40(BJ), (e) MP-MSU-1-4.0-40(BJ), and (f) MP-MSU-1-5.0-40(BJ). For the sake of clarity, the isotherms have been offset by 200 $cm^3\ g^{-1}$ along the volume adsorbed axis.

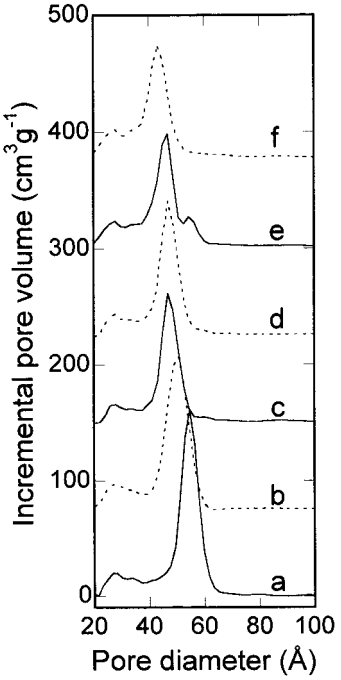

Figure 7. Pore size distributions for MSU-1 and its functionalized derivatives formed using Brij-76 as structure-directing surfactant at 40 °C: (a) MSU-1-40(BJ), (b) MP-MSU-1-1.0-40(BJ), (c) MP-MSU-1-2.0-40(BJ), (d) MP-MSU-1-3.0-40(BJ), (e) MP-MSU-1-4.0-40(BJ), and (f) MP-MSU-1-5.0-40(BJ).

of the excess TEOS and MPTMS that is not sequestered inside the micelles to form a clear solution. The less than quantitative synthesis yields obtained for the materials concur with the apparent loss of TEOS and/or MPTMS

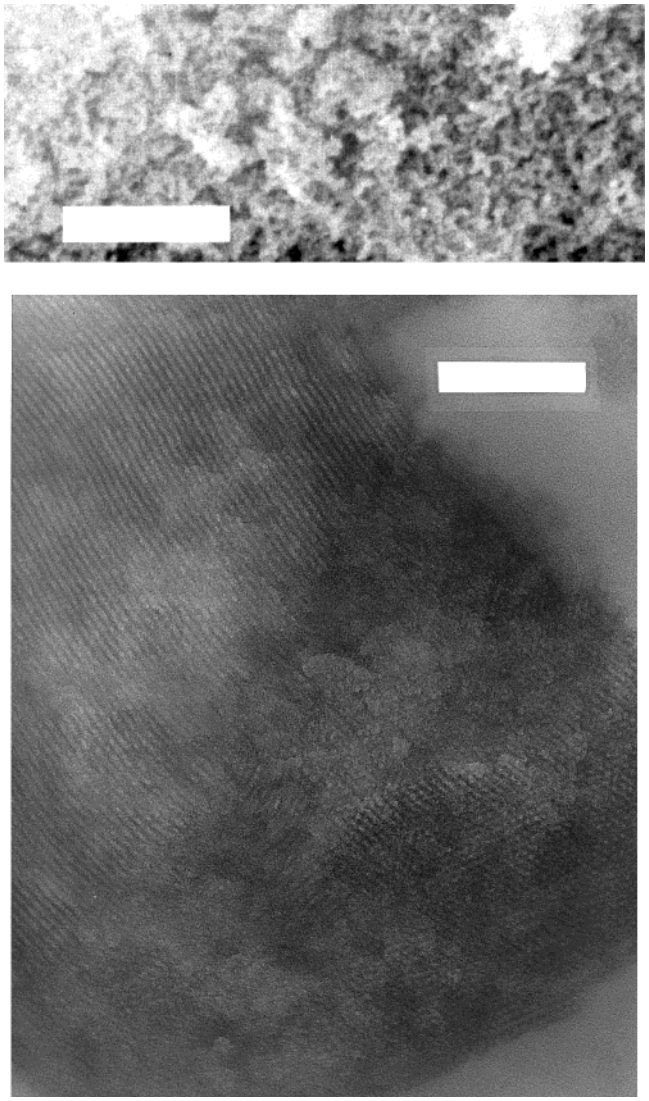

Figure 8. Electron micrographs of a mesostructure (MP-MSU-1-2.0-40(BJ)) assembled at 40 °C using Brij-76. Top: low resolution image obtained by scanning electron microscopy (scale bar = 10 μm). Bottom: high resolution image obtained by transmission electron microscopy (scale bar = 100 nm).

by evaporation (adjusting the pH of the synthesis mixtures' mother liquors to 9−10 by ammonia addition did not precipitate any product, suggesting that no unreacted silane precursors remained in solution). Attempts at synthesizing similar materials in covered beakers using otherwise identical reaction conditions resulted in the formations of materials with no long-range order or uniform porosity, although the yields of these amorphous products were nearly quantitative. Unlike the open-beaker syntheses, the silane−surfactant solution mixture did not clarify, but gradually formed product over the course of 3−4 days of stirring even without the addition of fluoride. Using neutral pH assembly conditions, the evaporation of excess silane thus appears to be crucial in obtaining precursor mesophases suitable for the controlled assembly of uniform-diameter mesostructures.

Since organosilanes such as MPTMS are likely to be somewhat more hydrophobic than TEOS, it follows that MPTMS may be preferentially partitioned from a TEOS/MPTMS mixture into the hydrophobic core of the micelles, resulting in a remaining TEOS:MPTMS molar

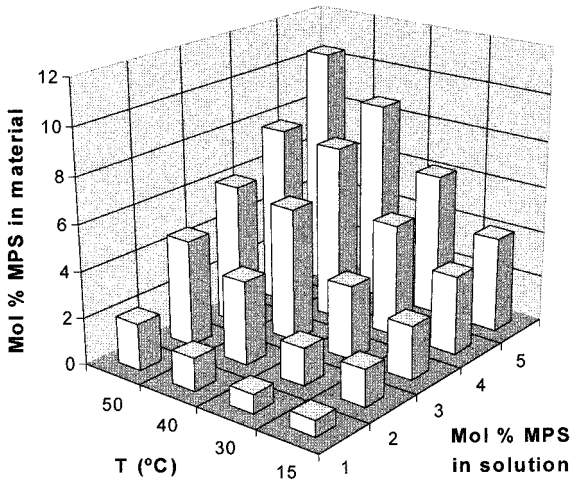

Figure 9. Effect of synthesis mixture composition (in TEOS and MPTMS) and temperature on MP-MSU-2 organosilane (MPS) group content for mesostructures prepared using Igepal CA-720 as the assembly surfactant.

ratio which is different from that of the original synthesis mixture. Hence, the cross-linking of the silanes at the surfactant−water interface by fluoride addition (viz., the poly(ethylene oxide) corona of nonionic surfactants is amphiphilic and provides a junction at which aqueous fluoride ions can interact with TEOS and MPTMS) forms mesostructured materials whose compositions reflect that of the micelle-partitioned MPTMS and TEOS precursors (and not necessarily that of the *original* synthesis mixture). At higher synthesis temperatures, the swelling of the hydrophobic cores of the micelles increases the overall hydrophobicity of the surfactant solution, thus further enhancing the partitioning of MPTMS into the micelles. As a result, the materials produced from higher temperature syntheses become enriched in MPS compared to those made at lower temperature.

The aforementioned temperature-dependent partitioning of MPTMS inside the micelles is further supported by the excellent correlation ($R^2 = 1.0$) observed between the mean degree of MPS incorporation in *all* of the MP-MSU-X materials prepared and the synthesis temperature (Figure 10).

It has been proposed that the assembly of mesostructures using nonionic surfactants under neutral pH conditions proceeds by the prehydrolysis of the silane precursors (TEOS), plausibly catalyzed by the increased nucleophilicity of water molecules bound to the oxygens along the poly(ethylene oxide) chains of the surfactants (i.e., the surfactant corona).[11] Although this process may be occurring during the formation of the materials presented in this work, this is not likely to be a controlling factor in the structure and composition of MP-MSU mesostructures. That the compositions and yields of the mesostructures do not correspond to the amount of silanes initially added to the synthesis mixtures is highly suggestive that loss of TEOS and MPTMS by evaporation must be occurring prior to any extensive precursor hydrolysis and cross-linking in the synthesis mixture.

Effect of Synthesis Parameters on Framework Structure. Figures 1 and 5 illustrate the effect of increasing MPS group content on the XRD patterns of

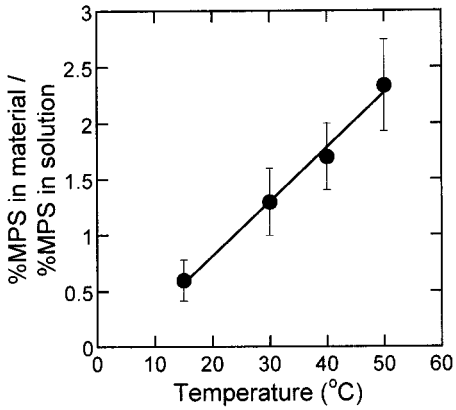

Figure 10. Correlation between average MPS incorporation (expressed as the MPS content of the mesostructures (column 4 in Tables 1−4) divided by the MPS added in the initial reaction mixtures (column 3, Tables 1−4)) and synthesis temperature for all mesostructures prepared from 15 to 50 °C. The error bars represent the standard deviation around the mean.

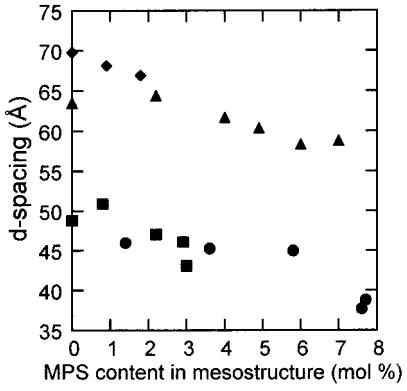

Figure 11. *d* spacings as a function of MPS group content in mesostructures prepared at 40 °C using Igepal CA-720 (●), Tergitol 15-S-12 (■), Triton-X100 (◆), and Brij-76 (▲) as the assembly surfactants.

a series of functionalized mesostructures prepared using Igepal CA-720 and Brij-76, respectively, at a synthesis temperature of 40 °C. As evidenced by the gradual shifting of the XRD correlation peak to higher angles of diffraction upon increasing MPS group loading, the *d* spacings of the mesostructures systematically decreased as a function of increasing MPS group content (Figure 11). These observations denote that lattice contractions occur as a result of the addition of organosilane into the mesostructures, and that the presence of such groups in the structures somewhat perturbs their crystallinity, although long-range order is nonetheless maintained in most of the mesostructures up to relatively high loading levels. We postulate that, being more hydrophobic than TEOS, the MPTMS molecules penetrate more deeply within the hydrophobic core of the micelles than does TEOS alone. Thus, when fluoride is added to hydrolyze and cross-link the silane precursors, the mesostructure thus formed possesses a smaller *d* spacing than would otherwise be obtained without the addition of any MPTMS.

In the case of the Igepal CA720 assembled mesostructures, the XRD correlation becomes gradually broadened as the materials become increasingly functionalized with the MPS moieties (Figure 1), denoting that the addition of organosilane into the surfactant solution slightly perturbs the structure of the assembly micelles. Similar trends in *d* spacings and peak breadth are observed for MSU-X materials prepared using the other surfactant systems (Tables 2−4). Only in the case of the MSU-2 mesostructures prepared using Triton-X100 as the assembly surfactant did significant structural perturbations arise upon the addition of more than 1 mol % MPTMS to the synthesis mixtures, resulting in materials which generally showed no diffraction signals in their XRD patterns (Table 3). The pore volumes of the latter were also markedly lower than those of their ordered counterparts (Table 3), denoting the formation of amorphous MPS-functionalized silica frameworks. These amorphous derivatives, however, still possessed the high surface areas and uniform mesopore size distributions characteristic of their more ordered counterparts, making them akin to functionalized silica gels. In contrast with the wormhole-motif mesostructures, the XRD patterns of the highly ordered hexagonal Brij-76 assembled mesostructured prepared at 40 °C largely retained their order upon the incorporation of the MPS moieties, as evidenced by the retention of the higher order (110) and (200) reflections in the XRD patterns (Figure 5). The reduction in signal intensity in these MPS-loaded mesostructures can thus be attributed to contrast matching between the silica framework and the incorporated MPS groups of the samples.[21,34]

Generally, the *d* spacings of the purely siliceous mesostructures were found to systematically increase as a function of synthesis temperature (Tables 1−4). This observation concurs with previously reported research[12] and is consistent with the notion that the hydrophobic cores of the surfactant micelles are increased in size at higher temperature and produce mesostructures with greater lattice spacings. This temperature-induced lattice expansion is also apparent for the MPS-functionalized MSU-X derivatives (Tables 1−4). A comparison between the *d* spacings of MPS-loaded mesostructures which possess similar compositions but were synthesized at different temperatures (using the same surfactant system) reveals that those prepared at higher temperature generally have greater *d* spacings than those prepared at lower temperatures. For instance, MP-MSU-2-5.0-30(IG), MP-MSU-2-3.0-40-(IG), and MP-MSU-2-3.0-50(IG) are all similar in composition (5.8−6.2 mol % MPS) but have *d* spacings of 40.1, 45.0, and 51.9 Å, respectively, which increase as a function of their synthesis temperatures (30, 40, and 50 °C, respectively) (Table 1).

Effect of Synthesis Parameters on Surface Properties and Porosity. Figures 2 and 6 illustrate the effect of increasing functional group loading on the N_2 isotherms of the mesostructures. The shift in the position of the isotherm inflections of the mesostructures to lower P/P_0 values (Figures 2 and 6) denotes a systematic decrease in pore diameters as a function of MPS incorporation (Figures 3 and 7). Moreover, the pore volumes of the mesostructures are found to diminish concurrently with their pore diameters (Tables 1−4). The decrease in pore diameter and volume can be attributed to both the occupancy of the pore channels by the incorporated MPS groups and the previously discussed lattice contraction resulting from the MPS incorporation.

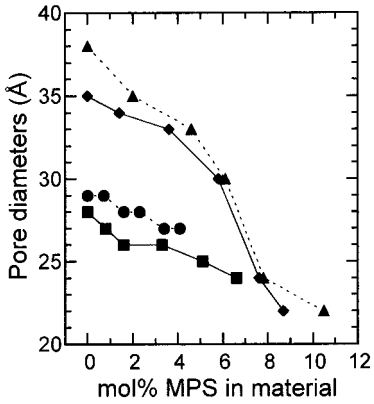

Figure 12. Pore diameters as a function of MPS group content for mesostructures prepared using Igepal CA-720 as the structure-directing surfactant at 15 °C (●), 30 °C (■), 40 °C (◆), and 50 °C (▲). The lines connecting the dots are meant as a guide to the eye.

Figure 12 illustrates the reduction of pore diameters for a series of functionalized mesostructures prepared at various temperatures. At low synthesis temperatures (15 and 30 °C), a gradual decline in the diameter of the mesostructures is observed as the MPS loading in the material increases, resulting from the presence of the organic groups on the pore channel walls, as well as from the lattice contraction caused by increased MPS loading (Figure 11). Owing to the increased size of the hydrophobic micelle cores at elevated temperatures, the materials with low (or no) MPS group loading (<∼6%) prepared at higher synthesis temperatures generally have significantly larger pore diameters than those prepared at lower temperature, an observation which is consistent with the previously discussed effect of temperature on mesostructure *d* spacing.[12] A precipitous decline in pore diameter, however, is denoted in the materials prepared at higher temperatures (40 and 50 °C) when these become highly loaded with MPS moieties (>∼6%, Figure 11). Such a decline in pore diameter is associated with concomitant reductions in both surface area and pore volume (Tables 1 and 4). It can be proposed that the dissolution of such relatively large amounts of MPS (which is more hydrophobic than TEOS) into the micelles results in a very deep penetration of organosilane molecules into the hydrophobic cores of the micelles, resulting in mesostructures with very reduced pore diameters, surface areas, and pore volumes. At lower micelle-partitioned MPS/TEOS molar ratios (below about 0.06), the MPS molecules do not "dive" as deeply into the micelle core, and essentially behave in a manner identical with that of the TEOS molecules.

It is noteworthy to mention that the incorporation of more than 6 mol % MPS was only possible in the cases of the Igepal and the Brij surfactant systems. The materials produced using either Triton-X or Tergitol 15-S-12 produced mesostructures devoid of long-range order at MPS loadings greater than 5%.

Conclusions

This work has explored the relation between various synthesis parameters (namely, temperature, relative reagent stoichiometry, and assembly surfactant) on the structure and composition of thiol-functionalized ordered mesoporous silicas prepared under neutral pH conditions. The composition, framework structure, and pore dimensions of the resulting materials were found to depend not only on the composition of the original reaction mixture, but also on the synthesis temperature. Hence, the simultaneous variation of both of these synthesis parameters was found to affect the amphiphilic character of nonionic surfactant structure directors, and provided a unique means of fine-tuning both the structure and the composition of organically functionalized mesostructures. We believe that these findings have provided new insights into the mechanistic issues involved in the formation of this interesting class of mesostructured materials. Further investigation, however, will be required in order to adequately elucidate the actual formation mechanisms of MSU-X mesostructures prepared under neutral pH synthesis conditions.

Acknowledgment. The authors thank the Natural Science and Engineering Research Council of Canada (NSERC) and Laurentian University for financial support. We also thank Dr. Glenn Facey (University of Ottawa NMR Lab) for providing NMR spectra of the samples. Dr. Neil Coombs (Imagetek Analytical Imaging, Toronto, Canada) is also gratefully acknowledged for TEM services.

CM010295V